

Electron Fermi surface of semimetallic alloys $\text{Bi}_{1-x}\text{Sb}_x$ ($0.23 \leq x < 0.56$)

N. B. Brandt, R. Hermann, G. I. Golysheva, L. I. Devyatkova, D. Kusnik, W. Kraak, and Ya. G. Ponomarev

Moscow State University

(Submitted 25 March 1982)

Zh. Eksp. Teor. Fiz. 83, 2152–2169 (December 1982)

The electron Fermi surface of semimetallic alloys $\text{Bi}_{1-x}\text{Sb}_x$ was experimentally investigated in the composition interval $0.23 \leq x < 0.56$. A monotonic increase of the Fermi-surface volume in L was observed with increasing x . It is established that the angle of inclination of the electron ellipsoids in the basal plane decreases linearly with increasing x . Data are obtained which indicate that the holes of the investigated samples are located at H extrema, just as in pure antimony. It is shown that the transformation of the electron Fermi surface of $\text{Bi}_{1-x}\text{Sb}_x$ alloys in the entire composition range $0 \leq x \leq 1$ can be described successfully by the model of McClure and Choi provided that a number of parameters of the model depend on the composition x .

PACS numbers: 71.25.Hc

INTRODUCTION

Bismuth and antimony, which form a continuous series of solid solutions $\text{Bi}_{1-x}\text{Sb}_x$ in the range $0 \leq x \leq 1$, are typical semimetals.¹⁻⁵ A characteristic feature of $\text{Bi}_{1-x}\text{Sb}_x$ alloys is that they go over into the semiconducting phase in the concentration range $0.07 \leq x \leq 0.22$ (Refs. 6–9). Semiconducting $\text{Bi}_{1-x}\text{Sb}_x$ alloys can be classified as narrow-band materials, since their thermal gap does not exceed 30 meV. Detailed calculations of the band structure of bismuth and antimony^{1,2} have made possible a qualitative understanding of why the alloys go over into the semiconducting phase in a narrow interval of the concentrations x (Refs. 10 and 11). Calculations^{1,2} have shown that the terms that determine the tops of the valence bands of bismuth and antimony have different symmetries. With increasing antimony concentration x , the top of the valence band (the term $T_{\bar{4}3}$) shifts rapidly downward in energy and reaches the bottom of the conduction band at $x = 0.07$ (Ref. 6). In the course of the elimination of the band overlap, the terms that determine at the point L the bottom of the conduction band and the top of the valence band become inverted, and this causes the transition of the alloys into the gapless state at $x \approx 0.04$ (Refs. 10 and 11).

The rearrangement of the band structure in the $\text{Bi}_{1-x}\text{Sb}_x$ alloys with increasing x in the ranges $0 \leq x \leq 0.22$ has by now been sufficiently well studied.⁶⁻¹⁹ At the same time, there are practically no data on the band structure of the alloys in the composition interval $0.22 \leq x \leq 0.75$. We still do not know the symmetry of the term that determines the top of the valence band of the alloys in the region of the semiconductor–semimetal transition ($x = 0.22$). In the composition interval $0.75 \leq x \leq 1$, as shown convincingly in Ref. 20, the hole parts of the Fermi surface are located at the points H of the reduced Brillouin zone (just as in pure antimony^{2,21}).

The electron Fermi surface of bismuth consists of three quasi-ellipsoids that have different axes and are centered relative to the points L and rotated away from the basal plane by an angle $\theta = +6^\circ 21'$ (Refs. 1 and 5). A dispersion law that describes in best fashion the entire aggregate of the existing experimental data was proposed for the bismuth carri-

ers at L by McClure and Choi.^{22,23} Their dispersion equation was obtained with the aid of the $\mathbf{k} \cdot \mathbf{p}$ method and contains a large number of parameters $Q_{ij}(\alpha_{ij})_{c,v}$ and P_{ijkl} , which manifest themselves respectively in first, second, and third orders of perturbation theory^{22,23}:

$$\varepsilon_+ \varepsilon_- = f, \quad (1)$$

where

$$\varepsilon_+ = \varepsilon + (\varepsilon_{gL} + \alpha_{v11}k_x^2 + \alpha_{v22}k_y^2 + \alpha_{v33}k_z^2 + 2\alpha_{v23}k_y k_z) / 2,$$

$$\varepsilon_- = \varepsilon - (\varepsilon_{gL} + \alpha_{c11}k_x^2 + \alpha_{c22}k_y^2 + \alpha_{c33}k_z^2 + 2\alpha_{c23}k_y k_z) / 2,$$

$$f = Q_{11}^2 k_x^2 + Q_{22}^2 k_y^2 + Q_{33}^2 k_z^2 + P_{2222} k_y^4 + P_{2223} k_y^3 k_z + (P_{2233} k_z^2 + P_{1122} k_x^2) k_y^2.$$

Here \mathbf{k} is the wave vector reckoned from the point L , the x axis is parallel to the binary axis, the y axis makes an angle $6^\circ 21'$ with the bisector direction, the z axis makes an angle $6^\circ 21'$ with the trigonal axis, ε_{gL} is the direct gap in L , the energy ε is reckoned from the middle of the gap in L , and the subscripts v and c correspond to the valence and conduction bands. The parameters Q_{ij} characterize the $\mathbf{k} \cdot \mathbf{p}$ interaction of the valence and conduction bands. The parameters α_{ij} , which are reciprocal correction masses ($\alpha_{ij} = m_0/m_{ij}$), take into account the effect of the four additional bands at L on the curvatures of the valence and conduction bands. It follows from symmetry that all the off-diagonal elements α_{ij} , with the exception of α_{23} , are equal to zero. The parameters α_{ij} can be either positive or negative. All that remain in f are the terms containing P_{ijkl} , in which k_y enters raised to the maximum powers (k_y^2, k_y^3, k_y^4). The reason for the latter is that k_y corresponds to the elongation direction, so that these terms should have the maximum values.

The dispersion law (1) is written in the atomic system of units: $e = m_0 = \hbar = 1$, the energy unit is one Hartree = 27.2 eV, and the length unit is the Bohr radius $a_B = 0.529 \text{ \AA}$.

All the constant parameters ($Q_{ij}, \alpha_{ij}, P_{ijkl}$) in (1) are empirical and are determined from a comparison of theory with experiment.

Owing to the strong interaction between the valence band and the conduction band in the x and z directions (the

TABLE I. Parameters of the electron dispersion law of bismuth and antimony (the values of Q_{ii} , α_{ij} , and P_{ijkl} are given in the atomic system of units).

Parameter	Bismuth ²³	Bismuth ^{26*}	Antimony, present work ^{**}
ϵ_F , meV	29.4	30.2±0.1	140.5±10 (129.5)
ϵ_{gL} , meV	-11.4	-(9±2)	180±30 (219)
Q_{11}	0.455	0.451±0.005	0.296±0.01
Q_{22}	0.0322	0.034±0.001	0.01±0.01
Q_{33}	0.342	0.340±0.005	0.355±0.01
α_{v22}	0.735	1.15±0.05	1.0±0.3 (1.15)
α_{c22}	0.676	0.66±0.03	0.67±0.01 (0.66)
α_{c23}	0.145	—	—
P_{1122}	-15.9	—	7±2
P_{2233}	-17.0	—	3.4±0.3
P_{2223}	—	—	2.1±0.2

*The parameters were determined within the framework of the dispersion law (2).

**The parameters indicated in parentheses were obtained from expressions (7), (10), (11), and (12).

parameters Q_{11} and Q_{33} are large), the terms containing $(\alpha_{11})_{c,v}$ and $(\alpha_{33})_{c,v}$ can in principle be left out under the condition that the energy ϵ does not penetrate too far into the interior of the conduction band or the valence band. At the same time, the parameter Q_{22} is anomalously small, so that at least terms with $(\alpha_{22})_{c,v}$ should be retained. Table I lists the parameters obtained by McClure and Choi^{22,23} for bismuth via comparison of the theory with Édel'man's⁵ precise data.

In the case when only the integrated characteristics of the electron Fermi surface are of interest, it is possible to use successfully the simplified McClure dispersion law²⁴

$$\begin{aligned} & (\epsilon + \epsilon_{gL}/2 + \alpha_{v22}k_y^2/2) (\epsilon - \epsilon_{gL}/2 - \alpha_{c22}k_y^2/2) \\ & = Q_{11}^2k_x^2 + Q_{22}^2k_y^2 + Q_{33}^2k_z^2. \end{aligned} \quad (2)$$

In the change from the dispersion law (1) to the dispersion law (2), all the terms that appear in third-order perturbation theory were left out, as well as the terms containing $(\alpha_{11})_{c,v}$, $(\alpha_{33})_{c,v}$, and $(\alpha_{23})_{c,v}$. With decreasing Fermi energy $\epsilon_F = |\epsilon| - |\epsilon_{gL}/2|$ and of the modulus of the gap parameter $|\epsilon_{gL}|$, Eqs. (1) and (2) go over into the Lax dispersion law (simple two-band model)²⁵:

$$\epsilon^2 - (\epsilon_{gL}/2)^2 = Q_{11}^2k_x^2 + Q_{22}^2k_y^2 + Q_{33}^2k_z^2. \quad (3)$$

Near the bottom of the conduction band or near the top of the valence band in L , as $|\epsilon_{gL}| \rightarrow 0$, the shape of the equal-energy surface approaches an ellipsoid, and the anisotropy of the electron and hole Fermi surfaces practically coincide and are determined by the anisotropy of the matrix elements Q_{ij} (see (3)) (in the latter case one speaks of the "mirror reflection" of the electron and hole spectra). Within the framework of the Lax model, the square of the cyclotron mass on the Fermi level, $m_c^2(\epsilon_F)$, increases linearly with increasing corresponding extremal section S . At a magnetic-field orientation $\mathbf{H} \parallel y$, it follows from (3) that

$$(m_{c \min}/m_0)^2 = S_{\min}/\pi Q_{11}Q_{33} + \epsilon_{gL}^2/4Q_{11}^2Q_{33}^2, \quad (4)$$

where $m_{c \min}$ is the maximum cyclotron mass on the Fermi level, m_0 is the mass of the free electron, and S_{\min} is the minimum cross section of the Fermi surface in L . As shown in Refs. 12, 26, and 27, for electrons and holes in L of bismuth and semiconducting $\text{Bi}_{1-x}\text{Sb}_x$ alloys, expression (4) is well satisfied at least in the interval $0 < \epsilon_F \leq 40$ meV. It follows therefore that in this range of the Fermi energy ϵ_F the influence of the remote bands on the dispersion of the electrons and holes in L in the direction of the short semi-axes (k_x, k_z) is negligibly small. At $(\alpha_{11})_{c,v}$, $(\alpha_{22})_{c,v} \neq 0$, with further increase of ϵ_F , the function $m_{c \min}^2 = F(S_{\min})$ may turn out to be nonlinear.

Despite the smallness of the gap parameter ϵ_{gL} of bismuth and of the alloys $\text{Bi}_{1-x}\text{Sb}_x$ ($0 < x < 0.15$), the influence of the remote bands on the dispersion the electrons in holes in L in the elongation direction (k_y of the equal-energy surfaces turns out to be quite noticeable (Q_{22} is small, see Table I). As a result of this influence, the holes in the y direction have a smaller transport mass than the electrons ($\alpha_{v22} > \alpha_{c22}$) (Table I).^{12,14,26} Because of this nonspecularity of the spectra, at equal ϵ_F and ϵ_{gL} , the anisotropy of the hole equal-energy surfaces is smaller than the anisotropy of the electron surfaces ($\epsilon_F, \epsilon_{gL} \neq 0$).^{12,26} The anisotropy of the electron and hole quasi-ellipsoids in L of the semiconducting alloys $\text{Bi}_{1-x}\text{Sb}_x$, where $\epsilon_{gL} > 0$, decreases monotonically with increasing Fermi energy.¹²

Comparison of a large number of experimental data makes it possible to conclude that for a $\text{Bi}_{1-x}\text{Sb}_x$ alloy with a "normal" spectrum (i.e., at $\epsilon_{gL} > 0$), no saddle point is realized in the spectrum; this is possible only if $\alpha_{v22}, \alpha_{c22} > 0$ (Table I). A saddle point in L can be obtained in principle for bismuth ($\epsilon_{gL} < 0$) under pressure (the modulus of the gap parameter ϵ_{gL} increases with increasing pressure²⁸) or for semiconducting $\text{Bi}_{1-x}\text{Sb}_x$ alloys ($\epsilon_{gL} > 0$) after they have been transferred to the region of the inverted spectrum ($\epsilon_{gL} < 0$) with the aid of pressure.²⁹

The antimony carrier density at helium temperatures exceeds by more than two orders of magnitude the carrier density in bismuth.²¹ The shapes of the three electron sections of the Fermi surface, centered (just as in the case of bismuth) about the points L of the reduced Brillouin zone, deviate noticeably from an ellipsoid.³⁰ The dispersion laws of the electrons and holes of antimony in L , in the directions of the short semi-axes of the energy surfaces, were described in Refs. 31 and 32 by using the Lax model²⁵ (i.e., an equation of the type (3) was assumed). The possibility of using Eq. (1) for the electrons and holes in L for antimony has not been investigated to this day. Nonetheless, it is clear from general considerations that the terms that appear in (1) in third-order perturbation theory can cause at large values of k the characteristic deviations of the shape of the Fermi surface from ellipsoidal, which are observed experimentally in pure antimony.³

In this study we have experimentally investigated the Fermi surface of semimetallic $\text{Bi}_{1-x}\text{Sb}_x$ alloys in the composition interval $0.23 \leq x \leq 0.56$ and attempted to describe the restructuring of the energy spectrum of the carriers in the $\text{Bi}_{1-x}\text{Sb}_x$ alloy system in the entire interval $0 \leq x \leq 1$ on the

basis of the McClure and Choi dispersion law (1).²²⁻²⁴ A monotonic increase of the volume of the electron Fermi surface was observed in L in the range $0.23 \leq x \leq 0.56$. In the composition interval $0.23 \leq x \leq 0.36$ the electron Fermi surface can be described in first-order approximation by a three-ellipsoid model. The angle of inclination of the electron ellipsoids to the basal plane decreases linearly with increasing x . Data are obtained indicating that the holes of the investigated alloys are located at H extrema, just as in pure antimony. It is shown that the carrier dispersion in L of pure antimony is satisfactorily described by the model of McClure and Choi.^{22,23} The parameters in the dispersion law (1) are calculated from the experimental data known for pure antimony.^{21,30-32} It is also shown that the restructuring of the electron Fermi surface of the $\text{Bi}_{1-x}\text{Sb}_x$ alloys, in the entire interval $0 \leq x \leq 1$, can be successfully described by the model of McClure and Choi under the condition that a number of parameters of the models depend on the composition x .

MEASUREMENT PROCEDURE. SAMPLES

The basic method of investigating the Fermi surface of the semimetallic alloys $\text{Bi}_{1-x}\text{Sb}_x$ ($0.23 \leq x \leq 0.56$) used in the present study was the Shubnikov-de Haas effect. The Shubnikov oscillations of the magnetoresistance $\rho(H)$ and of the first derivative $\partial\rho(H)/\partial H$ were written down in the magnetic-field range $0 \leq H \leq 55$ kOe at temperatures $1.9 \text{ K} < T < 4.2$ as the magnetic field was rotated in the binary-bisector ($\mathbf{H} \parallel C_3$) and bisector-trigonal ($\mathbf{H} \parallel C_2$) planes. Singlecrystal samples of the alloys were placed at the center of a superconducting solenoid in a drum-type rotating device. The sample rotation angle θ relative to the direction of the magnetic field \mathbf{H} was determined accurate to $\pm 0.10^\circ$ with an induction transducer connected in a follow-up system. The signal $\sim 1/H$, as well as the signal $\sim \pm \alpha H \pm \beta H^2$, used to suppress the monotonic behavior of $\rho(H)$ or $\partial\rho(H)/\partial H$, was generated with the aid of analog computing devices. The electric voltages proportional to θ , H , and $1/H$ were fed to digital volt-

meters. The signal $\propto \rho(H)$, after subtracting the signal $\propto \rho(0)$ and the monotonic component, was amplified by an F118/1 photoelectric amplifier. To record the Shubnikov oscillations of $\partial\rho(H)/\partial H$ we used a standard modulation technique. The signal $\propto \partial\rho(H)/\partial H$ was fed to a narrow-band amplifier and to a phase detector. In the latter case, the monotonic component was subtracted at the output of the phase detector. The Shubnikov oscillations of $\rho(H)$ or $\partial\rho(H)/\partial H$ were recorded in a magnetic field of either direction using an automatic x - y plotter.

The $\text{Bi}_{1-x}\text{Sb}_x$ single crystals were prepared by zone melting. The rate of motion of the zone was chosen such as to exclude the possibility of a cellular substructure as a result of concentrational supercooling. The composition of the $\text{Bi}_{1-x}\text{Sb}_x$ alloys was determined by x-ray microprobe analysis.

Rectangular samples with the typical dimension $0.5 \times 0.5 \times 3$ mm were cut along the binary axis C_2 from the single-crystal blanks by an electric-spark setup. The trigonal axis C_3 and the bisector were directed perpendicular to the lateral faces of the sample. After etching the sample in a polishing etchant and washing in ethyl alcohol, current contacts were soldered to the end faces of the samples with Wood's alloy. The potential contacts made of tinned copper wire ($50 \mu\text{m}$ diameter) were welded to the central part of the sample at a distance 0.5 mm from one another by electric-spark welding. Altogether we investigated 12 samples of $\text{Bi}_{1-x}\text{Sb}_x$ alloys in the composition range $0.23 \leq x < 0.56$ (Table II).

EXPERIMENTAL RESULTS

The Shubnikov oscillations of the magnetoresistance of the $\text{Bi}_{1-x}\text{Sb}_x$ alloys were recorded in the present study in both longitudinal ($\mathbf{H} \parallel \mathbf{j}$) and transverse ($\mathbf{H} \perp \mathbf{j}$) configurations. All the characteristic oscillation features possessed by pure bismuth were observed in this case^{33,34}:

1) At equivalent orientations of the magnetic field, on going from the longitudinal ($\mathbf{H} \parallel \mathbf{j}$) to the transverse ($\mathbf{H} \perp \mathbf{j}$)

TABLE II. Principal parameters of the electron Fermi surface in L for the $\text{Bi}_{1-x}\text{Sb}_x$ alloys investigated in the present study.

x	$\varepsilon_g L$, meV	Δ_1^{-1} , kOe ($\mathbf{H} \parallel C_2 \parallel \mathbf{x}$)	Δ_2^{-1} , kOe ($\mathbf{H} \parallel \mathbf{z}$)	Δ_3^{-1} , kOe ($\mathbf{H} \parallel \mathbf{y}$)	m_{c1}/m_0 ($\mathbf{H} \parallel \mathbf{x}$)	m_{c3}/m_0 ($\mathbf{H} \parallel \mathbf{y}$)	θ^* , deg	sample
0.23 ± 0.02	43.4 ± 5	19.7 ± 0.3	16.0 ± 0.2	1.2	—	0.005 ± 0.0005	4.0 ± 0.5	1-1
0.269	52.3	70.0 ± 1.0	56.2 ± 0.5	5.5	—	—	3.7 ± 0.5	1-2
0.27	52.6	80.0 ± 1.0	64.0 ± 1.0	6.1	—	0.0059 ± 0.0015	3.8 ± 0.5	1-3
0.275	53.7	74.5 ± 1.0	62.5 ± 1.0	5.49	—	0.0066	3.8 ± 0.5	1-4
0.276	53.9	85.5 ± 1.0	67.2 ± 1.0	6.8	0.166 ± 0.03	0.0081 ± 0.0012	3.6 ± 0.5	1-5
0.294	58.0	131.0 ± 2.0	93.5 ± 3.0	10.2	0.185 ± 0.03	0.0097 ± 0.0013	2.8 ± 0.5	1-6
0.334 ± 0.02	67.1 ± 5	206.7 ± 2.0	148.0 ± 3.0	18.6	0.204 ± 0.03	0.0137 ± 0.0015	2.3 ± 0.5	1-7
0.362 ± 0.025	73.5 ± 6	300.0 ± 8.0	230.0 ± 10.0	31.4 ± 2	—	0.0152 ± 0.0020	2.7 ± 0.5	1-8
0.368 ± 0.025	74.9 ± 6	321.6 ± 9.0	268.0 ± 10.0	37.0 ± 2	—	—	2.1 ± 0.5	1-9
0.496 ± 0.02	104.1 ± 5	—	—	96.0 ± 5	—	0.0282 ± 0.004	—	1-11
0.544 ± 0.03	115.0 ± 7	—	—	118.0 ± 5	—	0.0329 ± 0.003	1.5 ± 0.7	1-12
0.558 ± 0.03	118.2 ± 7	—	—	132.2 ± 7	—	0.0334 ± 0.003	—	1-13

configuration, the phase of the $\rho(H)$ oscillations changed by 180° ; when the successive quantum Landau level was detached from the Fermi level, the magnetoresistance $\rho(H)$ passed through a maximum at $\mathbf{H} \parallel \mathbf{j}$ and through a minimum at $\mathbf{H} \perp \mathbf{j}$.

2) The temperature dependence of the amplitude of the Shubnikov oscillations of $\rho(H)$ in the longitudinal configuration ($\mathbf{H} \parallel \mathbf{j}$) had an anomalous character—the amplitude of the oscillations decreased when the temperature was lowered from 4.2 to 1.9 K. At $\mathbf{H} \perp \mathbf{j}$ the amplitude of the oscillations increased with decreasing temperature in the standard manner.³⁵

It is known that the longitudinal ρ_{\parallel} and transverse ρ_{\perp} magnetoresistances (neglecting the anisotropy of the material at $\mathbf{H} = 0$) are expressed in terms of the component of the conductivity tensor $\sigma_{ij}(H)$ at $\mathbf{H} \parallel \mathbf{z}$ with the aid of the equations³⁵

$$\rho_{\parallel} = \sigma_{zz}^{-1}, \quad \rho_{\perp} = \sigma_{xx} / (\sigma_{xx}^2 + \sigma_{xy}^2).$$

When the next Landau level emerges σ_{zz} goes through a minimum and σ_{xx} through a maximum. For pure bismuth and pure $\text{Bi}_{1-x}\text{Sb}_x$ alloys, where $N = P$, we have $\sigma_{xy} \ll \sigma_{xx}$, so that when the Landau level is detached ρ_{\parallel} reaches a maximum value and ρ_{\perp} a minimum.^{33,34} If bismuth or $\text{Bi}_{1-x}\text{Sb}_x$ is doped by donor (Te, Se) or acceptor (Sn, Pb) impurities ($N \neq P$), the inverse inequality holds, $\sigma_{xy} \gg \sigma_{xx}$. In this case both ρ_{\parallel} and ρ_{\perp} go through a maximum when the quantum Landau level is detached from the Fermi level.^{12,26}

The anomalous temperature dependence of the amplitude of the Shubnikov oscillations of the longitudinal magnetoresistance ρ_{\parallel} of pure bismuth and of pure $\text{Bi}_{1-x}\text{Sb}_x$ alloys is due to the peculiarities of the interlevel phonon scattering at low temperatures.³³

Scattering by an ionized impurity predominates at helium temperatures in bismuth and in $\text{Bi}_{1-x}\text{Sb}_x$ alloys doped by donors or acceptors.^{12,26,27} The temperature dependence of the oscillation amplitude of the longitudinal magnetoresistance acquires in this case a classical character (just as in the de Haas–van Alphen effect).³⁵

It follows from the foregoing that the temperature dependence of the amplitude of the oscillations of the longitudinal magnetoresistance ρ_{\parallel} in the investigated pure $\text{Bi}_{1-x}\text{Sb}_x$ alloys can not be used to calculate the cyclotron masses of the carriers by the standard method. In the present paper the carrier cyclotron masses ($\mathbf{H} \parallel C_2$) were calculated by the usual procedure¹² at $\angle \mathbf{H} \cdot \mathbf{j} = 60^\circ$, where there were no anomalies whatever.

Quantum oscillations of the magnetoresistance $\rho(H)$ and of the derivative $\partial\rho(H)/\partial H$ were observed in all the investigated alloys in a wide range of angles when the magnetic field was rotated in the binary-bisector and bisector-trigonal planes. In accord with the character of the angular dependences of the oscillation frequency, the investigated samples of the $\text{Bi}_{1-x}\text{Sb}_x$ alloys can be arbitrarily divided into two groups. In the samples of the first group, with $0.23 \leq x \leq 0.35$, oscillations were observed only from the electron Fermi surface, while in the samples with $x > 0.35$ oscillations were observed both from the electron and from the hole Fermi sur-

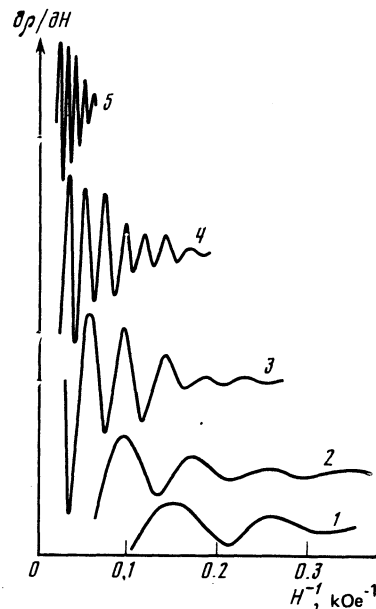


FIG. 1. Shubnikov oscillations of the derivative $\partial\rho(H)/\partial H$ at $\mathbf{H} \parallel C_2$ ($\angle \mathbf{H} \cdot \mathbf{j} = 60^\circ$) vs the close-to-minimum section of the electron Fermi surface in L at $T = 2.1$ K for samples of $\text{Bi}_{1-x}\text{Sb}_x$ alloys (Table II): 1—(1-4), 2—(1-6), 3—(1-7), 4—(1-8), 5—(1-11). The monotonic component of $\partial\rho(H)/\partial H$ is suppressed.

faces. It should be noted that the hole oscillations had as a rule a very small amplitude and were recorded reliably only in a narrow angle interval, so that the authors were unable to reconstruct fully the form of the hole Fermi surface. Nonetheless, the data obtained in the present paper allow us to state that the general character of the angular dependences of the hole-oscillation frequency in the investigated alloys agrees qualitatively with the analogous dependences of the frequency of the hole oscillations in pure antimony.²¹ The holes of the investigated alloys are located, with high degree of probability, at the H extrema (just as in pure antimony^{2,30-32}).

The frequency of the Shubnikov oscillations from the electron Fermi surface at L increase abruptly with increasing x (Fig. 1). In the composition range $0.23 \leq x \leq 0.35$, at $\mathbf{H} \parallel C_2$ and near this direction, high-frequency oscillations from the maximum S_{\max} and from the close-to-maximum sections of the electron Fermi surface at L were reliably registered.

In the angle interval $\angle \mathbf{H} C_2 = \pm 10^\circ$ the high-frequency oscillations from one of the electron ellipsoids and the low-frequency oscillations from the two other electron ellipsoids occur in different fields, so that the oscillations from the close-to-maximum cross sections become noticeable only in the region of the quantum limit for small cross sections (Fig. 2).

In an analogous situation, frequency modulation of the high-frequency oscillations is observed in pure bismuth and in n -type superconducting $\text{Bi}_{1-x}\text{Sb}_x$ alloys, owing to the strong motion of the Fermi level $\varepsilon_F(H)$ in a magnetic field.^{12,36,37} Beyond the quantum limit, for small sections of the Fermi surface at L , the frequency of the high-frequency oscillations from the near-maximum sections of the electron

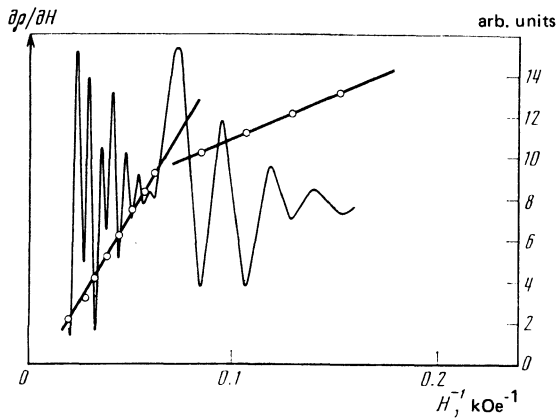


FIG. 2. Shubnikov oscillations of the derivative $\partial\rho(H)/\partial H$ at $H\perp C_3$ and $\angle HC_2 = 8^\circ$ at $T = 4.2$ K for sample 1-8. The monotonic component of $\partial\rho(H)/\partial H$ is suppressed.

Fermi surface can differ substantially from its "quasiclassical" value $\Delta^{-1} = cS_p eh$ (S_p is the extremal section of the Fermi surface in \mathbf{p} -space and Δ is the period of the oscillations in the reciprocal field).¹² In bismuth and in $\text{Bi}_{1-x}\text{Sb}_x$ alloys with $x < 0.12$, doped with an acceptor, the effect of frequency modulation of the high-frequency oscillations near the binary direction is much less pronounced, owing to the stabilizing action exerted on the Fermi level by the "heavy" holes in the T -extremum.^{6,12,26}

Our present detailed investigations of the dependence of the quantum number of the electronic high-frequency oscillations on the reciprocal field, $n(1/H)$, in a wide range of magnetic field (both below and above the quantum limit field for small sections) in the angle range $-15^\circ < \theta < +15^\circ$ near the binary direction, have shown that frequency modulation of the oscillations of the investigated pure $\text{Bi}_{1-x}\text{Sb}_x$ alloys is practically nonexistent. This experimental fact can be qualitatively explained in the following manner. In the angle interval $\angle HC_2 = \pm 15^\circ$, when the magnetic field is rotated in the binary-bisector plane, the small sections of four of the six pairwise equivalent hole quasi-ellipsoids at the H points are close in magnitude to the small sections of the two electron quasi-ellipsoids in L (Ref. 21). If the quantum-limit fields H_{ql} for the electron and hole quasi-ellipsoids are comparable in magnitude, the motion of the Fermi level in a magnetic field, $\varepsilon_F(H)$, in the ultraquantum region of magnetic fields at small cross sections, can turn out to be greatly weakened, since the electrons in L and the holes in H shift separately the Fermi level in opposite directions. Unfortunately, we were unable to verify this assumption by direct computer calculations (e.g., within the framework of the model of Smith, Baraff, and Rowell^{36,12}) for lack of data on the spin-splitting factor $\gamma = \Delta_{\text{spin}}/\Delta_{\text{orb}}$ for holes at the H points of the reduced Brillouin zone.

It was established in the present study that quantum oscillations from small sections of the electron Fermi surface in L have an integer phase (as $(1/H) \rightarrow 0$ the functions $n(1/H)$ are extrapolated to integer values of the quantum number). The latter indicates that the spin-splitting factor $\gamma = \Delta_{\text{spin}}/\Delta_{\text{orb}}$ for small sections of the electron equal-energy surfaces is close to unity.¹² We note that at $\gamma \approx 1$ the quan-

tum-limit field H_{ql} corresponding to the emergence of the doublet $(0^+, 1^-)$ practically coincides with the frequency Δ^{-1} of the oscillations from the given extremal section.

It follows from the theoretical calculations of McClure and Choi for a material such as bismuth that the charge carriers in L , at arbitrary orientation of the magnetic field, have a spin-splitting factor of the form²³

$$\gamma = 1 + \frac{|\varepsilon_{gL}|}{\varepsilon_{gL}} \left[\frac{m_c(\varepsilon_F)}{m_0} \right] K, \quad (5)$$

where K is a dimensionless function that depends little on the gap ε_{gL} , on the Fermi energy ε_F , and on the orientation of the magnetic field \mathbf{H} . The deviations of the factor γ from unity are determined to a considerable degree by the energy, gap, and angular dependences of the cyclotron mass $m_c(\varepsilon_F)$ on the Fermi surface. Bismuth and $\text{Bi}_{1-x}\text{Sb}_x$ alloys with $x < 0.04$, where the gap parameter $\varepsilon_{gL} < 0$, have a factor γ larger than unity for small sections of the electron Fermi surface and less than 0.5 for the maximum and medium sections.^{5,23} as $\varepsilon_F, \varepsilon_{gL} \rightarrow 0$ we have $\gamma \rightarrow 1$ at any orientation of the magnetic field. The latter leads, in particular, to a decrease in the spin-damping angle θ_{sd} in the semimetallic alloys $\text{Bi}_{1-x}\text{Sb}_x$ with increasing x in the interval $0 < x < 0.7$ (Ref. 15). The approach of the factor γ to unity for the maximum section of the Fermi surface in L as $\varepsilon_F \rightarrow 0$ was observed in semiconducting $\text{Bi}_{1-x}\text{Sb}_x$ alloys in Ref. 12.

It follows from (5) that the increment to unity reverses sign when the sign of the gap parameter ε_{gL} is reversed. Taking this circumstance into account, as well as considering the data for pure bismuth ($\varepsilon_{gL} < 0$),^{5,23} we can assume that in the $\text{Bi}_{1-x}\text{Sb}_x$ alloys investigated in the present study, where $\varepsilon_{gL} > 0$, the spin-splitting factor γ for small sections of the Fermi surface in L is less than unity (but remains close to unity). At the same time, the factor γ for the maximum and medium sections should be larger than unity. The alloys $\text{Bi}_{1-x}\text{Sb}_x$ in the composition interval $0.23 < x < 0.27$, revealed in the present investigation no spin-damping effect¹⁵ when the magnetic field was rotated in the binary-bisector plane near the binary direction, so that for the maximum cross section in the indicated interval of compositions we have $1 < \gamma < 1.5$. For $\text{Bi}_{1-x}\text{Sb}_x$ with $x > 0.27$, doubling of the frequency of the high-frequency oscillations from the near-maximum cross sections of the electron Fermi surface was observed in a narrow angle interval near $\mathbf{H}||C_2$; this doubling is possibly due to spin damping ($\gamma = 1.5$).

Calculation has shown that the angular dependences of the oscillation frequency $\Delta^{-1}(\theta)$ from the electron Fermi surface in L , in the case of the investigated alloys, are described satisfactorily within the framework of the three-ellipsoid model (Figs. 3 and 4). The inclination angle θ^* of the electron quasi-ellipsoids to the basal plane was determined by rotating the magnetic field in the bisector-trigonal plane ($\mathbf{H}||C_3$) (Figs. 3b and 4b). It was observed that θ^* decreases linearly (in first-order approximation) with increasing x (Fig. 5). Figure 5 shows also the data for pure bismuth,⁵ for semiconducting $\text{Bi}_{1-x}\text{Sb}_x$ alloys,¹² and for pure antimony.²¹ In the last case, the angle was taken between the normal to the minimum section and the bisector direction. We recall that

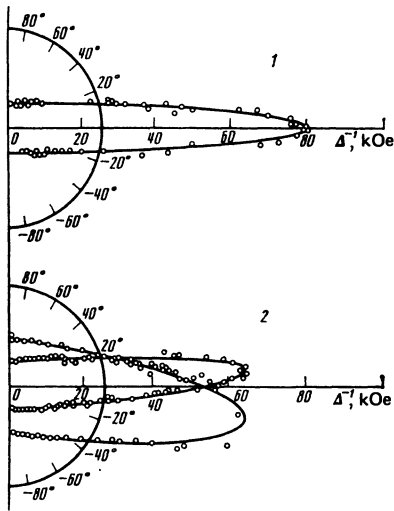


FIG. 3. Angular dependences of the frequency of the Shubnikov oscillations $\Delta^{-1}(\theta) \sim S_{\text{ext}}(\theta)$ from the electron Fermi surface in L of sample 1-3 upon rotation of the magnetic field in the binary-bisector (1) and bisector-trigonal (2) planes. The continuous lines are drawn in accordance with the three-ellipsoid model: 1) $\theta = 0$ at $\mathbf{H} \parallel C_2$, 2) $\theta = 0$ at $\mathbf{H} \parallel C_3$.

the signs of θ^* for bismuth and antimony are opposite.^{1,2}

An example of the angular dependence of the frequency of the Shubnikov oscillations from the hole Fermi surface when the magnetic field is rotated in the binary-bisector plane ($\mathbf{H} \perp C_3$) is shown in Fig. 4a (the corresponding branch is shown by the dashed curve). In the case of oscillations from small sections, the frequencies corresponding to the electron and hole Fermi surfaces were separated using a Fourier analysis and a computer. The character of the angular dependence of the hole-oscillation frequency at $\mathbf{H} \perp C_3$

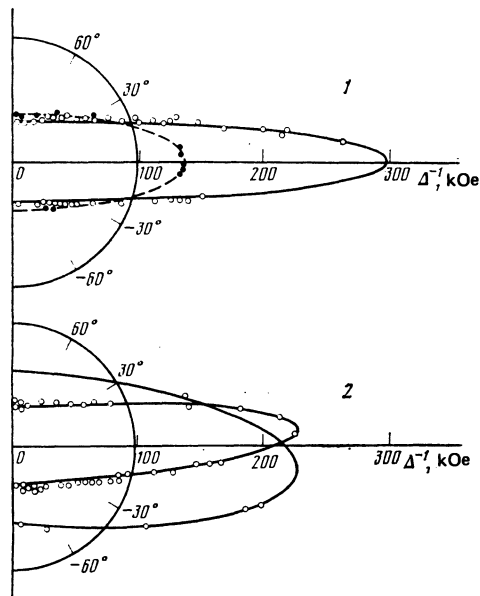


FIG. 4. Angular dependences of the frequency of the Shubnikov oscillations $\Delta^{-1}(\theta) \sim S_{\text{ext}}(\theta)$ from the electron (○) and hole (●) Fermi surfaces of sample 1-8 upon rotation of the magnetic field in the binary-bisector (1) and bisector-trigonal (2) planes: 1) $\theta = 0$ at $\mathbf{H} \parallel C_2$, 2) $\theta = 0$ at $\mathbf{H} \parallel C_3$.

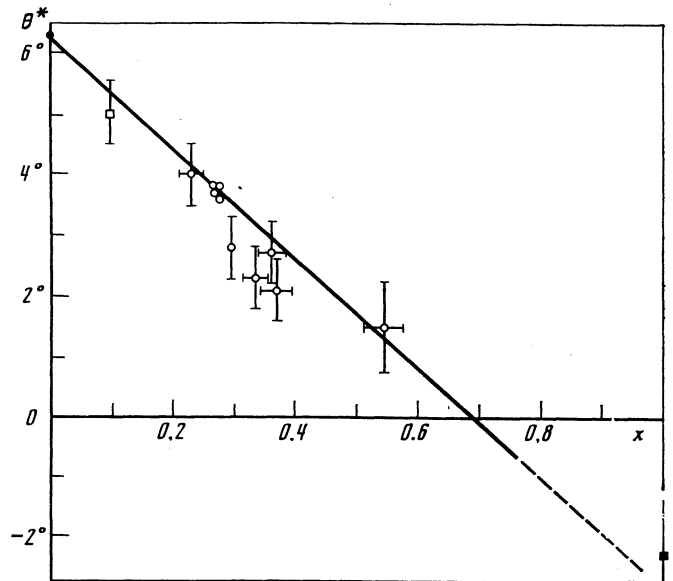


FIG. 5. Dependence on the composition x of the angle θ^* between the normal to the minimum section of the electron Fermi surface in L and the bisector for the alloys $\text{Bi}_{1-x}\text{Sb}_x$ ($0 < x < 1$): (○) present data, (●) Ref. 5, (□) Ref. 12, (■) Ref. 21.

agrees qualitatively with the character of the analogous dependence for the H holes in pure antimony.²¹

DISCUSSION OF RESULTS

The data obtained in the present paper (Table II) point to a smooth character of the rearrangement of the band structure of $\text{Bi}_{1-x}\text{Sb}_x$ alloys in the composition interval $0.22 < x < 1$. It was therefore of interest to ascertain whether the dispersion law (1) of McClure and Choi²²⁻²⁴ is suitable for the description of the energy spectrum of the carriers in L in the system of $\text{Bi}_{1-x}\text{Sb}_x$ alloys in the entire composition interval $0 < x < 1$. An analysis of the transformation of the Fermi surface of $\text{Bi}_{1-x}\text{Sb}_x$, with increasing x on the basis of Eq. (1), is impossible without reliable knowledge of the dependence of the gap parameter ε_{gL} on the composition x . A value $\varepsilon_{gL} = (-9 \pm 2)$ meV for bismuth at $T = 4.2$ K was obtained by Muller²⁶ (see also Ref. 23)). The $\varepsilon_{gL}(x)$ dependence in the composition interval $0 < x < 0.15$ was obtained by Tichovolski and Mavroides from magneto-optical measurements.¹¹ The dependence of the gap parameter ε_{gL} on the composition x , plotted from the results of Refs. 9, 11, 16, 17, and 26, is linear within the experimental error and is described by the empirical formula

$$\varepsilon_{gL} [\text{meV}] = (-9 + 228x). \quad (6)$$

From (6) it follows that $\varepsilon_{gL} = 219$ meV for pure antimony ($x = 1$). The possibility of using the linear approximation [Eq. (6)] in the entire range $0 < x < 1$ may raise some doubts. Unfortunately, at the present time there are no reliable data on the size of the gap ε_{gL} in L for pure antimony. The magneto-optical measurement data were not unambiguously explained because of the explicit absence of the Burstein effect.³

If the influence of the remote bands on the electron dispersion in the directions of the short semi-axes of the equal-

energy surfaces in L is neglected, the values of the gap ε_{gL} and of the product $Q_{11}Q_{33}$ for antimony can be determined from the dependence of $m_{c\min}^2$ on S_{\min} with the aid of expression (4). We have calculated ε_{gL} and $Q_{11}Q_{33}$ using experimental data for antimony doped with donors (Te) and acceptors (Sn).^{31,32} The values obtained were $\varepsilon_{gL} = 180$ meV and $Q_{11}Q_{33} = 0.105$. We note that the accuracy with which ε_{gL} is determined by these methods is low and amounts to ± 30 meV (Table I).

We have attempted in this study to determine for pure antimony the parameters that enter in the dispersion law (1) of McClure and Choi,^{22,23} using the angular dependences obtained for the Fermi wave vector $\mathbf{k}_F(\theta)$ from investigations of the radio-frequency size effect in antimony by Herrod, Gage, and Goodrich.³⁰

It was established that introduction into the simplified McClure dispersion law (2) of only three terms containing P_{2223} , P_{2233} , and P_{1122} and appearing in the third order of perturbation theory (see Eq. (1)) is sufficient for a satisfactory description of the electron Fermi surface of antimony. Figure 6 shows the experimental and theoretical angular dependences of the electron wave vector $\mathbf{k}(\theta)$ in the bisector-trigonal plane with the parameters contained in Table I. The theoretical curve *a* corresponds to a Fermi energy $\varepsilon_F = 140.5$ meV (the Fermi energy is reckoned from the bottom of the conduction band). The theoretical curves *b* and *c* were drawn respectively at $\varepsilon_F = 80$ and 20 meV. In all three cases $\varepsilon_{gL} = 180$ meV. As can be seen from Fig. 6, with decreasing Fermi energy the contribution of the terms containing P_{2223} , P_{2233} , and P_{1122} (see (1)) becomes weaker. In this case the shape of the electron Fermi surface becomes close to ellipsoidal, the angle between the normal to the maximum principal direction and the trigonal axis C_3 decreases rapidly, and the angle between the maximum and minimum cross sections approaches $\pi/2$.

Comparison of the parameters of the electron dispersion law, determined for pure bismuth and pure antimony (Table I), allows us to conclude the following. The parameters α_{v22} and α_{c22} , which take into account the influence of the remote bands on the dispersion law in the y direction, remain unchanged within the limits of error in the system of

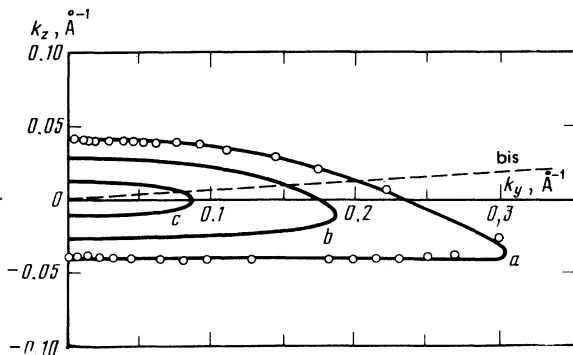


FIG. 6. Angular dependence of the Fermi wave vector \mathbf{k}_F of electrons in L for antimony (\circ) in the bisector-trigonal plane ($H1C_2$) according to the data of Ref. 30. Solid lines are drawn in accordance with (1) for the parameters given in Table I (third column): *a*— $\varepsilon_F = 140.5$, *b*— $\varepsilon_F = 80$, *c*— $\varepsilon_F = 20$ meV. In all three cases $\varepsilon_{gL} = 180$ meV.

alloys $\text{Bi}_{1-x}\text{Sb}_x$ in the entire range $0 \leq x \leq 1$. When x changes from zero to one, the parameter Q_{33} increases by $\sim 4\%$, and the parameter Q_{11} decreases by $\sim 34\%$. The parameter Q_{22} of antimony remains anomalously small; the accuracy of Q_{22} in the last case is very low.

The experimental data obtained in the present study were analyzed on the basis of the following empirical relations

$$Q_{11} = (0.451 - 0.155x) \quad (0 \leq x \leq 1), \quad (7)$$

$$Q_{33} = (0.340 + 0.015x) \quad (0 \leq x \leq 1), \quad (8)$$

$$\alpha_{v22} = 1.15 \quad (0 \leq x \leq 1), \quad (9)$$

$$\alpha_{c22} = 0.66 \quad (0 \leq x \leq 1), \quad (10)$$

$$\varepsilon = (-41.0 + 280.0x) \quad (0.22 \leq x < 0.6), \quad (11)$$

where $\varepsilon[\text{meV}] = \varepsilon_F + \varepsilon_{gL}/2$ is the electron energy reckoned from the center of the gap in L . The relation (11) presupposes a linear increase of ε in the interval $(0.22 \leq x < 0.6)$ and was obtained with account taken of (6). At $x = 0.22$ we have $\varepsilon = \varepsilon_{gL}/2$ (semiconductor–semimetal transition).

It has been assumed in the present study that the dependence of the gap ε_{gL} on the composition x is linear at least in the interval $0 \leq x < 0.6$ (i.e., expression (6) is valid in the indicated range of compositions). We recall that expression (6) overestimates somewhat the value of ε_{gL} for pure antimony (219 meV as against the value $\varepsilon_{gL} = 180$ meV that follows from calculations in accord with the data of Refs. 31 and 32).

The Fermi surface in L of the $\text{Bi}_{1-x}\text{Sb}_x$ alloys investigated in the present study was reconstructed fully only in the composition interval $x < 0.4$. At $x > 0.4$ the high-frequency oscillations from the maximum and next to maximum sections of the electron Fermi surface are shifted in fields $H > 60$ kOe, so that it was impossible to record them in our case. The estimate presented in this paper shows that for $\text{Bi}_{1-x}\text{Sb}_x$ with $x < 0.4$ the contribution made by the terms containing P_{ijkl} to the dispersion law (1) is quite small. When account is taken of the experimental errors it is possible, as shown by calculation, to remain within the framework of the Muller simplified dispersion law (2). In the latter case, for the principal sections of the Fermi surface in L and for the principal cyclotron masses on the extremal orbits, the following expressions are valid²⁴

$$S_{\min} = \pi(\varepsilon^2 - \varepsilon_{gL}^2/4)/Q_{11}Q_{33}, \quad (12)$$

$$m_{c\min}/m_0 = \varepsilon/Q_{11}Q_{33}, \quad (13)$$

$$S_{\max} = \frac{8(\varepsilon^2 - \varepsilon_{gL}^2/4)^{3/4} R^{1/2}}{3Q_{33}(\alpha_{v22}\alpha_{c22})^{1/4}} [BE(l) + (R-B/2)K(l)], \quad (14)$$

$$\frac{m_{c\max}}{m_0} = \frac{2\{EK(l) + F[2RE(l) + (B/2 - R)K(l)]\}}{\pi Q_{33}[\alpha_{v22}\alpha_{c22}(\varepsilon^2 - \varepsilon_{gL}^2/4)]^{1/4} R^{1/2}}, \quad (15)$$

$$S_{\max}/S_{\text{mid}} = m_{c\max}/m_{c\text{mid}} = Q_{11}/Q_{33}, \quad (16)$$

where

$$B = \frac{2Q_{22}^2 + (\varepsilon_{gL}/2)(\alpha_{v22} + \alpha_{c22}) + \varepsilon(\alpha_{c22} - \alpha_{v22})}{[\alpha_{v22}\alpha_{c22}(\varepsilon^2 - \varepsilon_{gL}^2/4)]^{1/2}} \quad (17)$$

$$R = (1 + B^2/4)^{1/2}, \quad F = (\varepsilon^2 - \varepsilon_{gL}^2/4)^{1/2}(\alpha_{v22} - \alpha_{c22})/2(\alpha_{v22}\alpha_{c22})^{1/2},$$

$K(l)$ and $E(l)$ are complete elliptic integrals of the first and

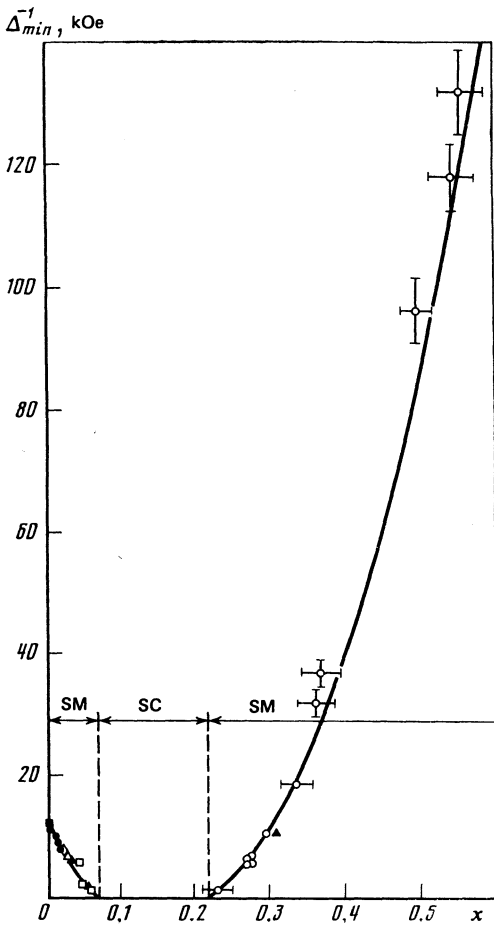


FIG. 7. Dependence of the Shubnikov oscillations frequency Δ_{\min}^{-1} from the minimum section S_{\min} of the electron Fermi surface in L on the composition x , for the alloys $\text{Bi}_{1-x}\text{Sb}_x$: (○) present study, (▲) Ref. 14, (■) Ref. 5, (●) Ref. 13, (□) Ref. 15, (△) Ref. 18, (◇) Ref. 39. The continuous curves are theoretical.

second kind, l is the modulus, and $l^2(\frac{1}{2}(B/2 + R)/R$.

Figure 7 shows the experimental plot, obtained in the present study, of the frequency Δ_{\min}^{-1} of the oscillations from the minimum section S_{\min} of the electron Fermi surface in L against the composition x , for the investigated $\text{Bi}_{1-x}\text{Sb}_x$ alloys in the composition interval $0.23 \leq x \leq 0.56$. The figure shows also a plot of $\Delta_{\min}^{-1}(x)$ for semimetallic $\text{Bi}_{1-x}\text{Sb}_x$ alloys with $x < 0.07$ according to data obtained by others. The continuous theoretical curve for $x > 0.22$, which is extrapolated to the value $\Delta_{\min}^{-1} = 682$ kOe at $x = 1$ (see Ref. 21), was obtained with the aid of Eqs. (6)–(8), (11) and (12). The continuous theoretical curve for $x < 0.07$ was plotted by solving the electroneutrality equation ($N = P$) with allowance for the dependence of the spectrum parameters on the composition x and under the condition

$$\varepsilon_{T_{45}} = (46.9 - 601.3x) \quad (x < 0.1), \quad (18)$$

where $\varepsilon_{T_{45}}$ [meV] = $\varepsilon_{ov} + |\varepsilon_{gL}|/2$ is the energy of the top of the valence band in T , reckoned from the center of the gap in L (ε_{ov} is the band overlap).

Figure 8 shows an experimental plot, against the alloy composition x , of the minimum cyclotron mass $m_{c \min}$ on the

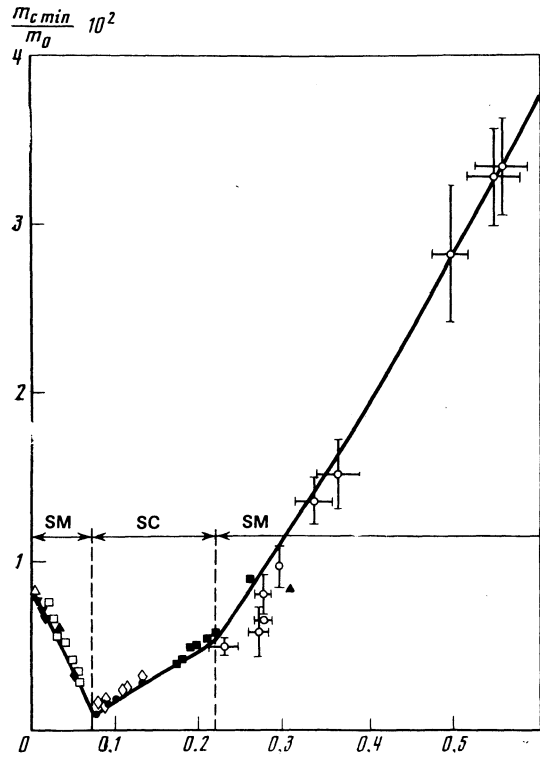


FIG. 8. Dependence, on the composition x , of the minimum electron cyclotron mass $m_{c \min}/m_0$ for $\text{Bi}_{1-x}\text{Sb}_x$ alloys: (○) present study, (■) Ref. 9, (▲) Ref. 14, (□) Ref. 19, (●) Ref. 17, (△) Ref. 5, (▼) Ref. 13, (◆) Ref. 40, (◇) Ref. 41. The continuous curves are theoretical.

Fermi level for the investigated alloys ($0.23 \leq x \leq 0.56$), and also plots of $m_{c \min}(x)$ ($x < 0.07$) and $m_{c \min}^0(x)$ ($0.07 < x < 0.22$) as obtained by others ($m_{c \min}^0$ is the minimum electron cyclotron mass at the bottom of the band for alloys in the semi-conducting phase). The solid theoretical curve at $x > 0.22$, which is extrapolated to $m_{c \min} = 0.84m_0$ at $x = 1$ (see Refs. 21 and 31), was obtained

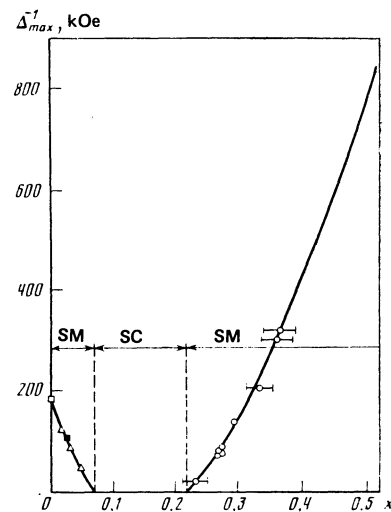


FIG. 9. Dependence, on the composition x , of the quasiclassical frequency of the Shubnikov oscillations Δ_{\max}^{-1} from the maximum section S_{\max} of the electron Fermi surface in L for the alloys $\text{Bi}_{1-x}\text{Sb}_x$: (○) present study, (□) Ref. 5, (■) Ref. 18, (△) Ref. 15. The continuous curves are theoretical.

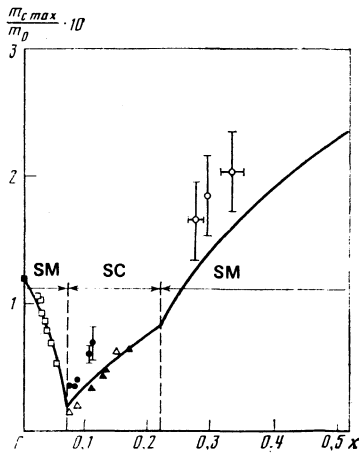


FIG. 10. Dependence on the composition x , of the maximum electron cyclotron mass $m_{c \max}/m_0$ for the alloys $\text{Bi}_{1-x}\text{Sb}_x$: (○) present study, (■) Ref. 5, (□) Ref. 19, (△) Ref. 16, (▲) Ref. 17, (●) Ref. 41. The continuous curves are theoretical.

with the aid of Eqs. (7), (8), (11), and (13). The solid theoretical curve in the region $0.07 < x < 0.22$ was drawn with the aid of (6), (8), and (13).

Figures 9 and 10 show plots, against the composition x , of the frequency Δ_{\max}^{-1} from the maximum section S_{\max} of the electron Fermi surface in L , and of the maximum cyclotron mass $m_{c \max}$, respectively. Figure 10 shows, in the interval $0.07 < x < 0.22$, the maximum electron cyclotron mass $m_{c \max}^0(x)$ on the bottom of the band. The theoretical curves in Figs. 9 and 10 at $x > 0.22$ were calculated from Eqs. (6)–(11), (14), and (15). The theoretical curves on Figs. 8–10 for $x < 0.07$ were obtained by solving the electroneutrality condition ($N = P$) under the condition (18).

From a comparison of the theory with the experimental data in the range $0 < x < 0.4$ in the present paper we have determined an empirical expression that describes the dependence of the small parameter Q_{22} on the composition x of the alloys $\text{Bi}_{1-x}\text{Sb}_x$:

$$Q_{22} = 0.0088 + 0.00126/(x+0.05) \quad (0 \leq x < 0.4). \quad (19)$$

Equation (19) is nonlinear. The abrupt decrease of Q_{22} as a

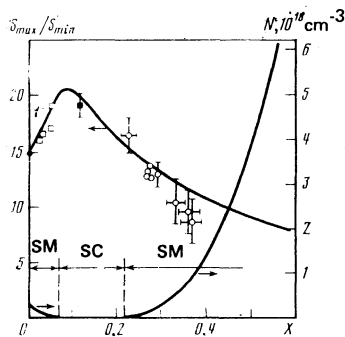


FIG. 11. Dependences, on the composition x of the anisotropy S_{\max}/S_{\min} of the electron Fermi surface and of the electron density N of the alloys $\text{Bi}_{1-x}\text{Sb}_x$: (○) present study, (●) Ref. 5, (■) Ref. 12, (□) Ref. 6. The continuous curves are theoretical (the anisotropy given for the alloys in the semiconductor phase, is that for the bottom of the conduction band).

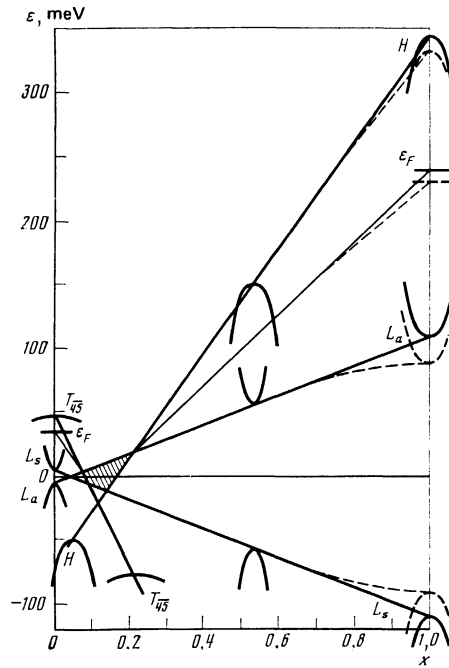


FIG. 12. Energy diagram of the restructuring of the spectrum of the alloys $\text{Bi}_{1-x}\text{Sb}_x$ ($0 < x < 1$). The continuous curves are drawn within the framework of the linear model (Eqs. (6)–(11) and (18)). The dashed lines at $x > 0.7$ are drawn with account taken of the values $\epsilon_{gL} = 180$ meV and $\epsilon_F = 140.5$ meV for antimony ($x = 1$) (see Table I).

function of x in the initial interval of the compositions brings the dispersion law (2) closer to the Abrikosov dispersion law proposed in Ref. 38.

Plots of the anisotropy of the electron Fermi surface S_{\max}/S_{\min} of the electron density N against the composition x are shown in Fig. 11. The value of N was calculated on the basis of the dispersion law (2) by numerical integration.

The data obtained in the present paper allows us to conclude that the restructuring of the electron energy spectrum in the $\text{Bi}_{1-x}\text{Sb}_x$ alloy system, in the entire interval $0 < x < 1$, can be successfully described on the basis of the theoretical model of McClure and Choi^{22–24} provided that a number of parameters of the model depend on the alloy composition x . The general character of the restructuring of the energy spectrum of the $\text{Bi}_{1-x}\text{Sb}_x$ alloys is illustrated by the diagram of Fig. 12.

In conclusion, the authors take the opportunity to thank A. B. Ormont and G. N. Ronami for a detailed analysis of the alloy composition with a microprobe analyzer. The authors are indebted to Professor J. W. McClure and to Dr. K. H. Choi for supplying the results of the theoretical calculation and for helpful discussions. The authors thank Professor J. R. Anderson and Professor H. D. Drew for stimulating discussions.

¹S. Golin, Phys. Rev. **166**, 643 (1968).

²L. M. Falicov and P. J. Lin, Phys. Rev. **141**, 562 (1966).

³M. S. Dresselhaus, J. Phys. Chem. Sol. **32** Suppl., 3 (1971).

⁴L. A. Fal'kovskii, Usp. Fiz. Nauk **94**, 3 (1968) [Sov. Phys. Usp. **11**, 1 (1968)].

⁵V. S. Edel'man, Usp. Fiz. Nauk **123**, 257 (1977) [Sov. Phys. Usp. **20**, 819 (1977)].

- ⁶G. A. Mironova, M. V. Sudakova, and Ya. G. Ponomarev, *Fiz. Tverd. Tela (Leningrad)* **22**, 3628 (1980) [*Sov. Phys. Solid State* **22**, 2124 (1980)].
- ⁷F. A. Buot, *J. Phys. Chem. Sol.* **32** Suppl., 99 (1971).
- ⁸N. B. Brandt, E. A. Svistova, and M. V. Semenov, *Zh. Eksp. Teor. Fiz.* **59**, 434 (1970) [*Sov. Phys. JETP* **32**, 238 (1971)].
- ⁹G. Oelgart, G. Schneider, W. Kraak, and R. Herrmann, *Phys. Stat. Sol. (b)* **74**, K75 (1976).
- ¹⁰S. Golin, *Phys. Rev.* **176**, 830 (1968).
- ¹¹E. J. Tichovolski and J. G. Mavroides, *Sol. St. Commun.* **7**, 927 (1969).
- ¹²G. A. Mironova, M. V. Sudakova, and Ya. G. Ponomarev, *Zh. Eksp. Teor. Fiz.* **78**, 1830 (1980) [*Sov. Phys. JETP* **51**, 918 (1980)].
- ¹³N. B. Brandt, L. S. Lyubutina, and N. A. Kryukova, *Zh. Eksp. Teor. Fiz.* **53**, 134 (1967) [*Sov. Phys. JETP* **26**, 93 (1968)].
- ¹⁴M. R. Ellett, R. B. Horst, L. R. Williams, and K. F. Cuff *J. Phys. Soc. Jpn.* **21** suppl., 666 (1966).
- ¹⁵B. A. Akimov, V. V. Moshchalkov, and S. M. Chudinov, *Fiz. Nizk. Temp.* **4**, 60 (1978) [*Sov. J. Low Temp. Phys.* **4**, 30 (1978)].
- ¹⁶G. Oelgart and R. Herrmann, *Phys. Stat. Sol. (b)* **58**, 181 (1973).
- ¹⁷G. Oelgart and R. Herrmann, *Phys. Stat. Sol. (b)* **79**, 501 (1976).
- ¹⁸W. Braune, G. Kuka, S. Hess, and H.-U Müller, *Phys. Stat. Sol. (b)* **79**, 501 (1977).
- ¹⁹W. Braune, G. Kuka, H.-J. Gollnest, and R. Herrmann, *Phys. Stat. Sol. (b)* **89**, 95 (1978).
- ²⁰D. V. Gitsu, F. M. Muntianu, and M. I. Onu, *Fiz. Nizk. Temp.* **3**, 1149 (1977) [*Sov. J. Low Temp. Phys.* **3**, 557 (1977)].
- ²¹L. R. Windmiller, *Phys. Rev.* **149**, 472 (1966).
- ²²J. W. McClure and K. H. Choi, *Sol. State Commun.* **21**, 1015 (1977).
- ²³K. H. Choi, *Dissertation*, Oregon State Univ., 1978.
- ²⁴J. W. McClure, *Low Temp. Phys.* **25**, 527 (1976).
- ²⁵B. Lax, *Bull. Am. Phys. Soc.* **5**, 167 (1960).
- ²⁶R. Myuller, Author's abstract of candidate's dissertation, Moscow State Univ., 1979.
- ²⁷N. B. Brandt, R. Myuller, and Ya. G. Ponomarev, *Zh. Eksp. Teor. Fiz.* **71**, 2268 (1976) [*Sov. Phys. JETP* **44**, 1196 (1976)].
- ²⁸M. Zigel', Author's abstract of candidate's dissertation, Moscow State Univ., 1981.
- ²⁹N. B. Brandt, H. Dittmann, Ya. G. Ponomarev, and S. M. Chudinov, *Pis'ma Zh. Eksp. Teor. Fiz.* **11**, 250 (1970) [*JETP Lett.* **11**, 160 (1970)].
- ³⁰R. A. Herrod, C. A. Gage, and R. G. Goodrich, *Phys. Rev.* **B4**, 1033 (1971).
- ³¹A. E. Dunsworth and W. R. Datars, *Phys. Rev.* **B7**, 3435 (1973).
- ³²G. A. Harte, M. G. Priestley, and J.J. Vuillemin, *J. Low Temp. Phys.* **31**, 897 (1978).
- ³³S. Tanuma and R. Inada, *Tech. Report of ISSP, ser. A., No. 658*, Japan, 1974.
- ³⁵L. M. Roth and P.N. Artyres, *Semiconductors and Semimetals*, A. K. Willardson and A. C. Beer, eds., Vol. 1, Academic, 1966, p. 159.
- ³⁶G. E. Smith, G. A. Baraff, and J. W. Rowell, *Phys. Rev.* **135**, A1118 (1964).
- ³⁷N. B. Brandt and L. G. Lyubutina, *Zh. Eksp. Teor. Fiz.* **47**, 1711 (1964) [*Sov. Phys. JETP* **20**, 1150 (1965)].
- ³⁸A. A. Abrikosov, *J. Low Temp. Phys.* **8**, 315 (1972).
- ³⁹P. W. Chao, H. T. Chu, and Y. H. Kao, *Phys. Rev.* **B9**, 4030 (1974).
- ⁴⁰G. E. Smith, *Phys. Rev. Lett.* **9**, 487 (1962).
- ⁴¹B. Fellmuth, H. Krüger, R. Rudolph, and R. Herrmann, *Phys. Stat. Sol. (b)* **104**, 209 (1981).

Translated by J. G. Adashko.